

1
2 **Microwave atmospheric pressure plasma jets for wastewater treatment:**
3 **Degradation of methylene blue as a model dye**

4
5 María C. García^{1,*}, Manuel Mora², Dolores Esquivel², John E. Foster³, Antonio Roderó⁴,
6 César Jiménez-Sanchidrián², Francisco J. Romero-Salguero^{2,*}

7
8 ¹Department of Applied Physics, University of Cordoba, Ed- C2, Campus de Rabanales, Córdoba, 14071, Spain

9 ²Department of Organic Chemistry, Fine Chemistry and Nanochemistry Research Institute, University of
10 Cordoba, Ed- C3, Campus de Rabanales, Córdoba, 14071, Spain

11 ³Department of Nuclear Engineering and Radiological Sciences, University of Michigan, Ann Arbor, Michigan,
12 48109, USA

13 ⁴Department of Physics, University of Cordoba, Ed- C2, Campus de Rabanales, Córdoba, 14071, Spain

14 * Authors to whom any correspondence should be addressed: Tel. +34957218638, e-mail: qo2rosaf@uco.es
15 (F.J.R.-S.); Tel. + 34957212633, e-mail: fa1gamam@uco.es (M.C.G.).

16 *Keywords:* atmospheric pressure plasmas; advanced oxidation processes; microwave
17 discharges; dye degradation; water treatments

18

19 **ABSTRACT**

20 The degradation of methylene blue in aqueous solution as a model dye using a non thermal
21 microwave (2.45 GHz) plasma jet at atmospheric pressure has been investigated. Argon has
22 been used as feed gas and aqueous solutions with different concentrations of the dye were
23 treated using the effluent from plasma jet in a remote exposure. The removal efficiency
24 increased as the dye concentration decreased from 250 to 5 ppm. Methylene blue degrades
25 after different treatment times, depending on the experimental plasma conditions. Thus,
26 kinetic constants up to 0.177 min^{-1} were obtained. The higher the Ar flow, the faster the
27 degradation rate. Optical emission spectroscopy (OES) was used to gather information about
28 the species present in the gas phase, specifically excited argon atoms. Argon excited species
29 and hydrogen peroxide play an important role in the degradation of the dye. In fact, the
30 conversion of methylene blue was directly related to the density of argon excited species in
31 the gas phase and the concentration of hydrogen peroxide in the aqueous liquid phase. Values
32 of energy yield at 50% dye conversion of 0.296 g/kWh were achieved. Also, the use of two
33 plasma applicators in parallel has been proven to improve energy efficiency.

34

35 **1. Introduction**

36 In recent times there has been a dramatic increase in the amount of organic pollutants
37 (volatile organic compounds, pharmaceuticals, organic dyes...) detected in water resources,
38 thus representing a serious concern for the public health. Among these contaminants, dye
39 wastewaters from the textile industry are particularly widespread (approx. 1 million kg of
40 dyestuffs are emitted into the environment per year) (Foster et al., 2012) and pose numerous
41 problems (affectation of photosynthesis in water plants, carcinogenicity, etc.). Consequently,
42 the removal of colour from textile industry wastewaters represents a major environmental
43 goal as it enables water reuse for further textile mill processing. However, dyes are designed
44 to resist degradation and so this is not an easy task. Indeed, the new organic dyes coming to
45 market have very stable molecular structures so conventional wastewater treatment techniques
46 are usually ineffective for their degradation. As a consequence, new technologies for removal
47 of dyes from wastewater have been investigated.

48 Advanced Oxidation Techniques and Processes (AOPs) are approaches allowing in situ
49 decomposition of organic compounds in water through mineralization, i.e. conversion of the
50 compound to carbon dioxide, water and inorganic intermediates (Glaze et al., 1987). AOPs
51 have been developed to generate hydroxyl free radicals by different techniques (Al-Kdasi et
52 al., 2004), and use these radicals as strong oxidants. More generally, the term AOP also refers
53 to chemical processes and precursors that have high reduction potentials and either produce
54 OH or directly attack organic molecules (ozone, atomic oxygen, excited nitrogen, ultrasound,
55 UV light, and peroxide) (Foster et al., 2012). AOPs have been proven to be powerful and
56 efficient treatment methods for degrading recalcitrant materials and toxic contaminants
57 (Mohajerani et al., 2009).

58 In the last years, plasmas have begun to be employed to induce AOPs for water
59 treatment purposes (Anpilov et al., 2001; Lukes et al., 2005; Sato and Yasuoka, 2008; Stratton

60 et al., 2015). More specifically, plasmas are sources of excited species, charged particles,
61 radicals and UV radiation, among others, each of which are themselves advanced oxidation
62 techniques (Foster et al., 2012). Different kinds of plasmas, using different configurations
63 have been employed for water (and other liquids) treatment (Malik, 2010), particularly for the
64 abatement of organic pollutants such as dyes (Clements et al., 1987; Yang et al., 2005;
65 Magureanu et al., 2007; Dojčinović et al., 2011; Reddy et al., 2013), phenolic compounds
66 (Sun et al., 2000; Krugly et al., 2015) and antibiotics (Magureanu et al., 2011; Kim et al.,
67 2015).

68 Nowadays non-thermal plasmas, i.e. those whose electron temperature is different from
69 the corresponding to ions and neutrals (gas temperature), are considered as a very promising
70 technology. Their non-equilibrium properties including low power consumption and their
71 ability to achieve enhanced gas phase chemistry at relatively low gas temperature, are
72 responsible for the great attention that these plasmas have gained from an applied point of
73 view and their extensive use in applications that require low temperatures, including material
74 processing and synthesis, biomedical applications, and surface modification, among others
75 (Park et al., 2001; Selwyn et al., 2001; Zille et al., 2015).

76 In particular, non-thermal atmospheric-pressure plasma jets/plumes play an increasingly
77 important role in various plasma-assisted applications for several reasons (Walsh et al., 2006;
78 Laroussi and Akan, 2007; Laroussi, 2009; Walsh et al., 2010; Lu et al., 2012). First of all, due
79 to their practical capability in providing plasmas which are not spatially confined by
80 electrodes and whose stability is not compromised by the presence of the sample to be
81 processed. Plasma jets are able to generate stable discharges in a gas and then flush it to a
82 separate region of reactive gas for processing applications (Walsh et al., 2006). This spatial
83 separation enables a considerable flexibility in jet designs in order to achieve a good control in
84 both plasma dynamics and reaction chemistry (Mora et al., 2010; Mora et al., 2011).

85 Secondly, because plasma jet configuration offers a chamberless delivery of downstream
86 reaction chemistry if desired (Walsh et al., 2010). Finally, they are free from constraints
87 imposed by vacuum-compatibility, as they operate at atmospheric pressure, being this an
88 undeniable advantage in practical applications.

89 Atmospheric plasma jets can be generated in many different gases and using different
90 electrical excitations. Several cold plasma jet devices have been designed; most of them are
91 described in Laroussi and Akam review (Laroussi and Akan, 2007) although there are others
92 more recently developed such as the plasmas generated by using nanosecond dc voltage
93 pulses with kilohertz repetition frequencies as well as with sine-wave excitations in the
94 kilohertz-to-megahertz range in pulsed or continuous mode (Chandana et al., 2015).

95 In the present work, we report for the first time on the design of a plasma jet reactor
96 allowing liquid (water) treatment based on the use of a microwave (2.45 GHz) surface wave
97 sustained discharge at atmospheric pressure (Ferreira and Moisan, 1993). This type of
98 discharge generates non thermal plasmas with a high electron density (in the order of 10^{14} cm^{-3}),
99 and so a high reactivity (Henriques et al., 2011b). Microwave discharge reactors enable the
100 generation of very stable and reproducible plasmas, that can operate over a broad range of
101 experimental conditions (pressure, gas type, frequency, power, geometry), so being capable to
102 produce copious and controlled amounts of active species. As far as the authors know, this is
103 the first study where a microwave plasma jet of this type have been employed for water
104 treatment.

105 More specifically, the reactor consisted of a plasma-jet over liquid configuration that
106 was employed for degradation of methylene blue in aqueous solution. Remote exposure of the
107 sample was done (Laroussi, 2009). In contrast to direct exposure (in which the sample is
108 subject to all possible agents generated by the plasmas including heat, charged particles,

109 reactive neutrals, and electromagnetic radiation), in remote exposure the effect of charged
110 particles on the water sample under treatment is weak as the sample is placed at some distance
111 from the plasma and most of these species recombine before reaching it. The heat flux is also
112 greatly reduced in this case, what leaves mainly the long-lived radicals to directly interact
113 with the sample (Laroussi, 2009).

114

115 **2. Experimental part**

116

117 *2.1. Chemicals*

118 Methylene blue (MB) was selected as the model organic *contaminant* dye because of its
119 stable molecular structure. Moreover, MB-laden waste water exhibit a high chroma and
120 toxicity and has become an unmanageable industrial wastewater (Wang et al., 2013) whose
121 treatment has being profusely studied in the last years. Methylene blue (Fig. S1) is a
122 heterocyclic aromatic compound belonging to the phenothiazine family (C₁₆H₁₈N₃SCl). It was
123 purchased from Sigma-Aldrich and used without further purification.

124

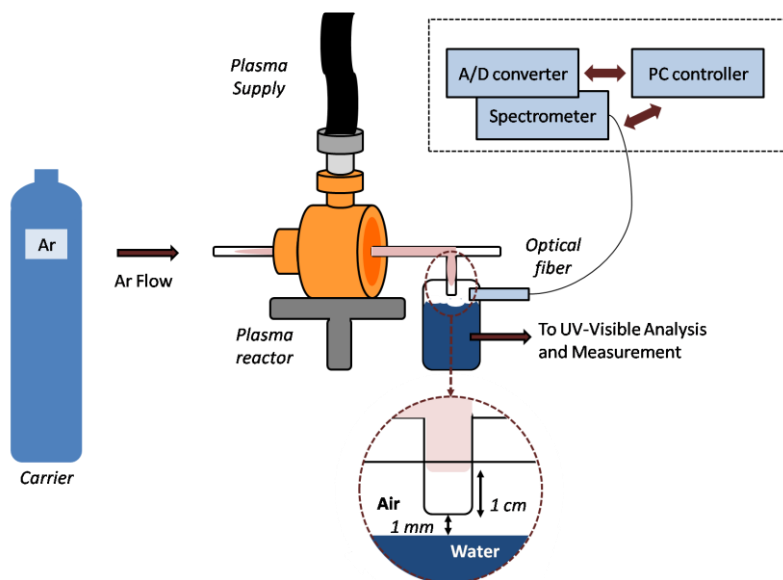
125 *2.2. Plasma reactor*

126 Fig. 1 shows the experimental set-up used for the generation of the plasma. A surfatron
127 device (Moisan and Pelletier, 1992) was used to couple the energy coming from a microwave
128 (2.45 GHz) generator (with a maximum stationary power of 200 W in continuous-wave
129 mode) to the support gas (argon with a purity ≥ 99.995 %) within a quartz reactor tube of 1.5
130 and 4 mm of inner and outer diameter, respectively, opened to the air as shown in Fig. 1.
131 Surfatron was originally designed to generate cylindrical plasma columns inside straight
132 dielectric tubes (Moisan and Pelletier, 1992), sustained by an azimuthally symmetric TM₀₀
133 surface wave mode (Henriques et al., 2011a). Nevertheless, in our experiments a T-shaped

134 tube with a closed end was employed in order to allow the plasma column go down through
135 the vertical part of the tube and approach the water.

136

137



138

139 **Fig. 1.** Experimental set-up for the generation of plasma and OES measurements

140

141 2.3. Methods

142 In this work, the microwave power was set at 150 W and the argon flow rate (adjusted
143 using a calibrated mass flow controller) ranged from 350 to 1400 sccm. The movable plunger
144 and stubs permitted the impedance matching so that the best energy coupling could be
145 achieved, making the power reflected back to the generator (P_r) negligible (< 5%).

146 Plasma effluent downstream was directed to a solution of methylene blue (MB) dye in
147 deionized water. The distance between the end of the plasma column and water was about 11
148 mm, so that the sample suffered a remote plasma exposure (did not come in direct contact
149 with the plasma at any time). Solutions with different MB concentrations (ranging from 5 to
150 250 mg/L) were treated.

151 MB decomposition was monitored as a function of treatment time. In all cases, the water
152 temperature never exceeded 55 °C. As shown in additional experiments, thermal degradation
153 of the dye was negligible under these experimental conditions.

154

155 2.4. Analysis

156 Optical Emission Spectroscopy (OES) techniques (sensitive, not invasive and very easy
157 to implement tools) were employed to identify plasma active species reaching the water and
158 triggering AOPs leading to dye degradation. Emission from the afterglow region next water
159 was side-on collected using an optical fiber, and analyzed by using a Czerny-Turner type
160 spectrometer of 1 m focal length equipped with a 2400 grooves/mm holographic grating and a
161 photomultiplier (spectral output interval of 200-750 nm) as a detector. Spectra were recorded
162 with a spectral resolution of 0.08 nm, and allowed us to gather information about different
163 species that reach the water.

164 The degradation of the dye was followed by UV–visible absorption spectroscopy. Foster
165 et al. (Foster et al., 2013) have shown that for methylene blue solutions this technique is a
166 reasonable diagnostic to track actual dye concentrations. UV–visible absorption spectra of
167 MB solutions before and after plasma treatment were measured by a spectrophotometer in the
168 wavelength range 250–800 nm. The absorbance is proportional to the concentration of
169 absorbing molecules, according to the Beer-Lambert law. The concentration of the dye in
170 solution was determined from the absorption maximum at 668 nm, which was also employed
171 for the calibration curves.

172 Conversion was calculated as:

$$173 \quad conv (\%) = \frac{C_0 - C}{C_0} \times 100 \quad (1)$$

174 where C_0 and C are initial and final concentrations of the MB solution, respectively.

175 The apparent kinetic constant (k) was determined by fitting to a pseudo first order
176 reaction:

$$177 \quad \ln\left(\frac{C_0}{C}\right) = kt \quad (2)$$

178 where t is the reaction time.

179 On the other hand, the energy yield, which measures the efficiency of the dye
180 degradation process, has been defined as the ratio between the amount of methylene blue
181 removed during plasma treatment and the consumed energy:

$$182 \quad \text{energy yield}(g/kWh) = Y = \frac{V(L) \times C_0(g/L) \times \text{conv}(\%)/100}{P(kW) \times t(h)} \quad (3)$$

183 where V is the methylene blue solution volume and P is the microwave power supplied.

184 Peroxide-test strips (0.5–25 mg/L Mquant, Merck) based on a colorimetric method were
185 used for H_2O_2 determinations, and changes of pH and conductivity were measured with a
186 Orion Star A329 (Thermo Scientific) digital meter. Test strips for ammonia (0.5-6.0 mg/L),
187 nitrate (10-500 mg/L) and nitrite (1-80 mg/L) from Macherey-Nagel were also used.

188

189 **3. Results and Discussion**

190 *3.1. OES spectra and plasma activated species*

191 The optical emission spectrum (Fig. S2) was measured downstream, 1 mm below the
192 end of the plasma tube (position of the aqueous solution, see Fig. 1). Although this position
193 was 11 mm distant from the end of the luminous plasma column and there was no apparent
194 emission from this region, OES spectrum revealed the presence of some argon atomic (Ar I)
195 system lines (696.54, 706.72, 738.40, 750.38, 763.51, 772.42 nm) corresponding to radiative
196 de-excitations from $4p$ and $4p'$ to $4s$ levels. Thus, the aqueous solution was placed at this
197 separate region where some plasma species were still active and provide chemical reactivity.
198 The plasma jet flushed out active species are able to reach the water.

199 Long-lived excited neutrals (argon metastables) should be likely the main energy
 200 carriers for generation of new reactive species in the remote region of this microwave plasma
 201 jet (Yu and Yasuda, 1998; Laroussi, 2009; García et al., 2010). At this region, pooling
 202 Penning reactions of metastable argon atoms can generate argon atoms, argon ions Ar^+ and
 203 argon dimer ions Ar_2^+ by means of metastable-metastable Ar^m ionization collisions and
 204 metastable-metastable associative ionization (García et al., 2010).



207 and recombination reactions of ions Ar^+ and Ar_2^+ produce argon excited atoms Ar^* , justifying
 208 the emission observed:



212 Although before reaching the water, plasma jet effluent came into contact with air,
 213 emission lines corresponding to species containing nitrogen or oxygen (such as N_2 , NO , $\text{O} \dots$)
 214 were not detected. Particularly, energetic argon metastables ($E \sim 11.5\text{-}11.8$ eV) are able to
 215 cause excitation of nitrogen molecules through nearly-resonant excitation transfer reactions
 216 leading to the emission of the Second Positive System ($\text{C}^3\Pi_u - \text{B}^3\Pi_g$), typical of atmospheric
 217 pressure argon plasma jets opened to the air (Jackson and King, 2003). The lack of these
 218 emissions is probably a residence time issue due to the high speed of the plasma effluent in
 219 this reactor (ranging between 3.3 and 13.2 m/s).

220 Optical emission spectroscopy techniques could not be used to measure plasma
 221 characteristic parameters such as electron density, electron temperature or gas temperature in
 222 this post-discharge region next to the water, because of the lack of emission of specific lines

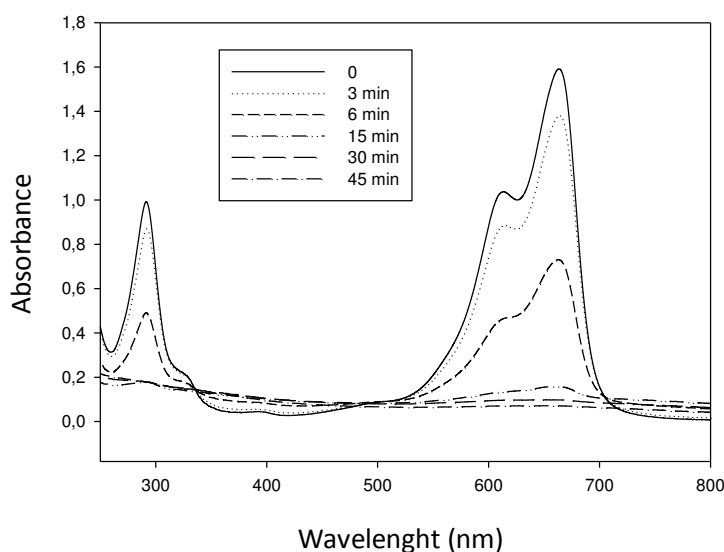
223 related to these diagnoses (Hydrogen Balmer Series lines or ro-vibrational bands of some
224 molecular species such as OH, N₂, CN...).

225

226 3.2. Influence of experimental conditions on the transformation of MB

227 The UV-visible spectra for an untreated MB solution and for plasma jet treated
228 solutions during different time intervals in the range 3–45 min are shown in Fig. 2. In these
229 experiments the initial dye concentration was 50 ppm, the solution volume was 40 mL and
230 argon (gas feeding the plasma) was ran at a flow rate of 1400 sccm in the discharge. The
231 absorption maxima intensity in the UV-visible spectra (at ca. 293, 609 and 668 nm) decreased
232 with increasing treatment time and the solution became colourless after 30 minutes exposure
233 to the plasma.

234



235

236 **Fig. 2.** UV-visible spectra for an untreated and plasma jet treated MB solution (50 ppm)
237 during different time intervals

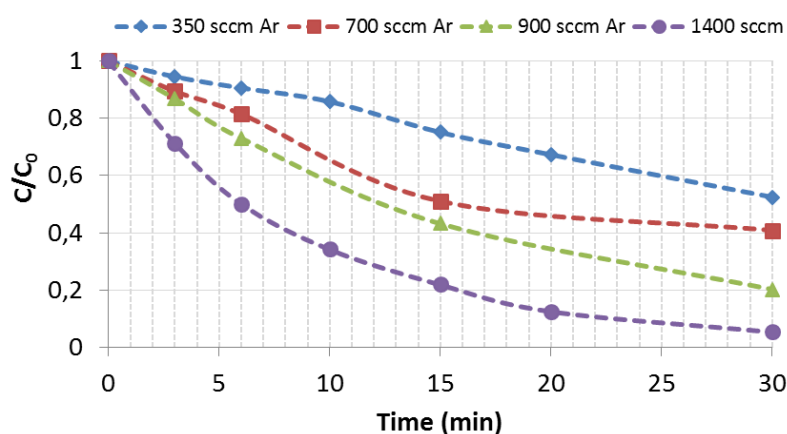
238

239 Argon flow rate also had an important effect on the degradation of the dye, as illustrated
240 in Fig. 3. The higher the argon flow rate, the faster the MB was decomposed. In order to

241 understand this fact, the intensity of Ar I line at 763.51 nm (proportional to the amount of
242 argon atomic excited species reaching the water) was monitored for different argon flow rates
243 (Fig.4). A linear increase was found as a result of the higher amount of plasma active species
244 reaching the aqueous solution per unit of time (*vide infra*). In the range of experimental
245 conditions studied, the energy efficiency of this reactor (measured from the energy yield at 50
246 % conversion) increased with the argon flow rate (Fig. S3).

247 Under the reaction conditions studied, methylene blue degradation followed a pseudo-
248 first-order kinetics. At an Ar flow rate of 1400 sccm, the apparent kinetic constant was 0.097
249 min^{-1} with a correlation coefficient (R^2) of 0.997. This value is in the range of those found in
250 the degradation of methylene blue in a pulsed tubular plasma reactor (Reddy et al., 2013) or
251 an atmospheric pressure non-thermal plasma jet (Chandana et al., 2015), ca. between 0.03 and
252 0.15 min^{-1} , and also in the degradation of reactive blue 19 in a needle-plate discharge system
253 in argon and air, 0.017 and 0.089 min^{-1} , respectively (Sun et al., 2016). Much lower values
254 (up to 0.014 min^{-1}) were reported in a pulsed discharge plasma combined with activated
255 carbon for the degradation of acid orange 7 (Guo et al., 2016).

256



257
258

259 **Fig. 3.** Degradation of the dye over time (MB concentration 50 ppm) for plasma treatments
260 using different argon flow rates

261

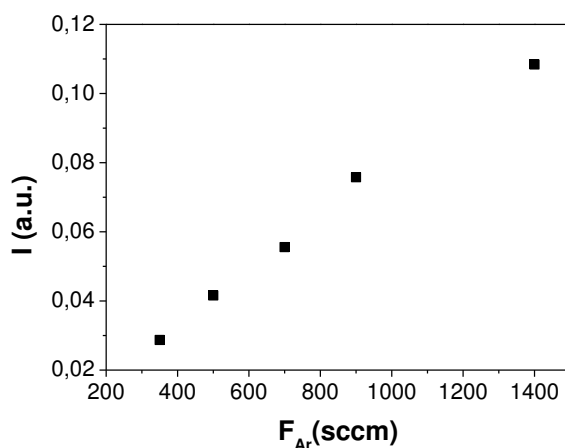


Fig. 4. Intensity of the Ar I line 763.51 nm measured next to the water for different argon flow rates

On the other hand, the possibility of improving plasma reactor efficiency in MB decomposition by operating with multiple plasma applicators in parallel was also investigated. For this purpose, a dual applicator using a sole surfatron was employed (Fig. S4). The source consisted of two identical quartz reactor tubes, and the total MW power injected to the system was kept at 150 W. The energy efficiency using dual-tube configuration (at 700 + 700 sccm) was much higher (with an energy yield at 50 % conversion of $Y_{50\%} = 0.037$ g/kWh) than single-tube configuration (at 700 sccm) efficiency ($Y_{50\%} = 0.012$ g/kWh).

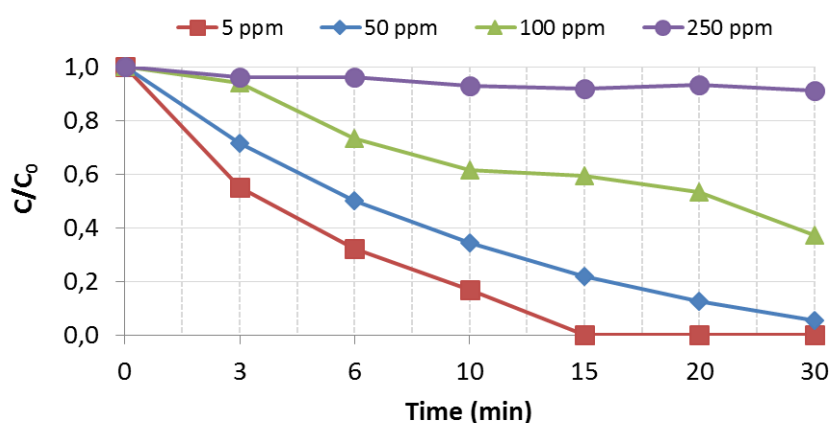
Similar MB transformation curves over time were obtained for single-tube configuration reactor working at 1400 sccm and dual-tube configuration working at (700 + 700) sccm. A similar result was found for 700 sccm and (350 + 350) sccm in single and dual-tube configurations, respectively. From these results it can be inferred that, in the range of the argon flow rate considered, the amount of species reaching water rather than their speed played the most relevant role in the MB decomposition process. The slightly higher efficiency of dual versus single configuration could be most likely ascribed to the larger volume of humid air affected by the plasma in the former case. Thus, the apparent kinetic constant was

281 0.118 min⁻¹ for dual-tube configuration working at (700 + 700) sccm, whereas it was 0.097
282 min⁻¹ for single-tube configuration reactor working at 1400 sccm.

283 The initial concentration of the dye in solution was another parameter affecting the MB
284 degradation rate. The relative decomposition of methylene blue decreased with increasing the
285 initial dye concentration (Fig. 5). Table 1 also illustrates that MB degradation at low dye
286 concentration is much more effective in terms of the energy yield. Also, the apparent kinetic
287 constant increased with the decrease in dye concentration from 0.097 min⁻¹ at 50 ppm to 0.177
288 min⁻¹ at 5 ppm. At higher concentrations, likely intermediates formed can interact with each
289 other and compete with dye decomposition (Zhu et al., 2014).

290 The degradation pathways of MB have been recently studied with hydroxyl radicals
291 being a key factor during the process. Several intermediate compounds have been detected by
292 demethylation, deamination and ring cleavage, among other reactions, and the resulting
293 mixture has been shown to be totally nontoxic (Huang et al., 2010; Bansode et al., 2017)

294
295



296
297 **Fig. 5.** Degradation of the dye over time for plasma treatments of MB aqueous solutions
298 of different initial concentrations (argon flow rate 1400 sccm).

299
300

301 **Table 1**302 Energy yield at 50 % conversion ($F_{Ar} = 1400$ sccm).

Dye concentration (ppm)	$Y_{50\%}$ (g/kWh)
5	0.296
50	0.033
100	0.018
250	0.007 ^a

303 ^a Maximum value registered (50% conversion was not reached)

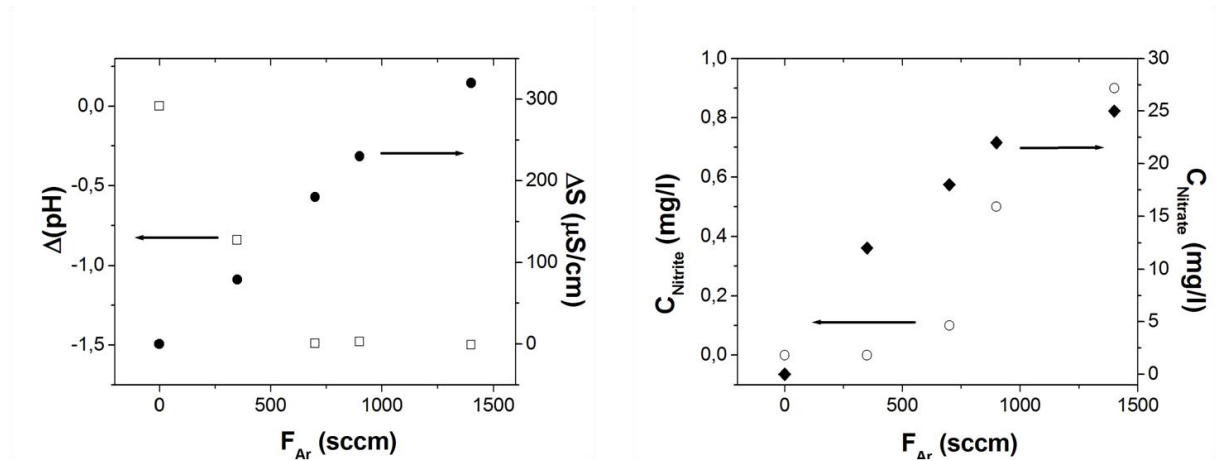
304

305 *3.3. Plasma jet influence on water properties*

306 In order to gain further insight into the chemical activity of this plasma reactor, changes
307 in deionized water properties induced by the application of the plasma afterglow were
308 investigated. Thus, the ability of this plasma reactor to generate H₂O₂, and the changes of pH
309 and conductivity in pure water caused by the treatment were studied. Since the most important
310 pathway for H₂O₂ formation is by combination of OH radicals, H₂O₂ is considered as an
311 indicator for hydroxyl radical formation in plasma in contact with water (Locke and Shih,
312 2011; Magureanu et al., 2013). These radicals are very active species able to degrade organic
313 pollutants. Plasma jet treatment generated H₂O₂ species in water in all the cases studied
314 (Table S1).

315 This plasma reactor was able to generate up to 5 mg/L of H₂O₂ after 30 min treatment
316 on a 40 mL water sample. This amount increased to 25 mg/L when the sample volume
317 reduced to 8 mL. These amounts are similar to those found in other discharge processes
318 (Yang et al., 2005). The energy yield for hydrogen peroxide formation for the most favourable
319 case studied ($F_{Ar} = 1400$ sccm) was 2.7 mg/(kW·h), falling in the range of the values reported
320 for different electric discharges above liquids (Locke and Shih, 2011). The generation rate in
321 this case was $4.1 \cdot 10^{-4}$ g/h.

322 Two experiments consisting of a pure chemical treatment, i.e., without plasma, were
 323 conducted to check the influence of H₂O₂ in the degradation of MB. They were carried out
 324 with H₂O₂ concentrations of 10 and 100 mg/L for the treatment of 50 mg/L of MB and
 325 revealed that there was no dye degradation under stirring for 30 min at room temperature.
 326



327
 328 **Fig. 6.** Changes of electrical conductivity and pH (left) and concentrations of nitrite and
 329 nitrate (right) in water after plasma treatment as a function of argon flow rate
 330

331 Conductivity of the water underwent an increase after plasma jet treatment as shown in
 332 Fig. 6, having again a linear dependence with argon flow rate. This result can be explained by
 333 the dissolution of species formed in the gas phase by the action of the plasma jet and
 334 subsequent hydrolytic reactions in the liquid phase leading to the generation of different ions.
 335 A small reduction of water pH was detected upon plasma jet exposure, also decreasing with
 336 argon flow rate. Species NO₂⁻ and NO₃⁻ were detected in water upon plasma treatment (see
 337 Fig. 6) and their formation usually involves an increase of the water acidity due to the
 338 concomitant formation of H₃O⁺ ions (*vide infra*). The measured concentration of both NO₂⁻
 339 and NO₃⁻ were in the range of those reported by other authors in different discharge plasmas
 340 in contact with water (Lukes et al., 2014). Moreover, ammonia was not detected in the water.
 341

342 *3.4. Formation of H₂O₂ species and methylene blue degradation*

343 Combinations of charged particles, ozone, hydrogen peroxide and UV radiation have
344 been shown as a way to produce hydroxyl radicals in water and to effectively degrade many
345 organic compounds (Lukes and Locke, 2005). Plasma is a source of all these species. Ozone
346 has been claimed to play an important role in the degradation of dyes (Yang et al., 2005).
347 However, ozone formation is practically suppressed in air due to the reaction of oxygen atoms
348 with nitrogen (Deng et al., 2013; Sun et al., 2016). In the present case, plasma jet mainly
349 delivers argon excited species, photons and heat at the remote region next to water. Argon
350 species (excited or metastables) striking on the water surface are likely leading to water
351 dissociation in hydroxyl and hydrogen radicals at the interface region (Magureanu et al.,
352 2008) (Fig. S5).



354 Also, as some water evaporation is expected, these reactions might also have taken
355 place at the gas phase consisting of humid air. In this region (gas phase), plasma jet species
356 should also be interacting with surrounding air molecules. Excitation transfer from argon
357 metastables to ground state of molecular nitrogen is the main mechanism provoking nitrogen
358 molecules excitation (Timmermans et al., 1998):



360 These species might cause further dissociation of water molecules (Magureanu et al., 2008):



362 OH species formed in the gas phase reach the water solvating, and so producing OH_{aq}.
 363 Finally, OH_{aq} species in water react in the presence of a third molecule to give hydrogen
 364 peroxide, eventually difusing to the bulk liquid (Locke and Shih, 2011) :



366 Since H₂O₂ itself did not degrade MB, as discussed above, OH radicals will most likely
 367 be the main reactive species responsible for the degradation of dye molecules. In the case of
 368 the dual-tube configuration, a greater contact with the humid air and a bigger generation of
 369 these species would explain the best efficiency for MB degradation of this approach.

370 On the other hand, the presence of nitrites and nitrates in treated water can be explained
 371 by reactions implying long-lived species N_xO_y generated in the gas phase (where plasma came
 372 in contact with air) solvating into the liquid (Lietz and Kushner, 2016). Reactions of N_xO_yaq
 373 (solvated) gave rise to formation of acids *HNO_xaq* and explain the observed decrease in pH
 374 upon the treatment with plasma (Lukes et al., 2014).



379

380 Finally, in order to gain an insight into the importance of these mechanisms, argon,
 381 nitrogen and synthetic air were added in the gas region in contact to the liquid surface. The
 382 external injection of argon gas into the region where the discharge makes contact with the
 383 liquid improves slightly the MB conversion, unlike air or nitrogen, thus suggesting the role of
 384 argon species in these processes (Fig. S6).

385 A linear dependence of the MB transformation on the density of Ar I (*4p*) species as
386 inferred from argon emission was observed (Fig. S7). This supports the outstanding role of
387 the abovementioned mechanism mediated by argon excited species. Thus, the larger the
388 concentration of excited argon species, the higher the transformation of MB.

389

390 **4. Conclusions**

391 In this work, the use of a microwave (2.45 GHz) plasma jet for treatment of MB-laden
392 water was investigated. Dye degradation was followed by UV–visible spectroscopy, and
393 Optical Emission Spectroscopy (OES) techniques (sensitive, non-invasive and very easily
394 implementable tools) were employed to identify plasma active species triggering AOPs
395 leading to dye degradation. The degradation of the dye methylene blue was more efficient at
396 low dye concentration. Also, an increase in the argon flow rate produced a higher degradation
397 rate and, in fact, the possibility of using two plasma applicators in parallel have been
398 demonstrated. Indeed, multiple applicators were found to be slightly more efficient than a
399 single applicator even with equal total flow and total input power. For sample volumes lower
400 or equal to 50 mL, values of energy yield at 50 % of dye conversion ranged between 0.033
401 and 0.296 g/kWh, among the best values reported in the literature (Sato and Yasuoka, 2008).
402 The plasma reactor was able to generate hydrogen peroxide species in pure water, whose
403 concentration increased with the plasma argon flow rate. For the most favourable case
404 studied, the energy yield for H₂O₂ formation was 2.7 mg/(kW·h), falling in the range of
405 values reported in the literature for different electric discharges above liquids (Locke and
406 Shih, 2011). Also, several experiments proved that argon excited species plays an important
407 role in the formation of the active species that at last degrade the organic pollutant.

408

409 **Acknowledgements**

410 The authors wish to acknowledge funding of this research by Spanish Ministry of Science and
411 Innovation (Project MAT2013-44463-R), Andalusian Regional Government (Project P10-
412 FQM-6181 and FQM-136 and FQM-346 groups) and Feder Funds.

413

414 **References**

415

- 416 Al-Kdasi, A., Idris, A., Saed, K., Guan, C.T., 2004. Treatment of textile wastewater by
417 advanced oxidation processes—a review. *Global nest: the Int. J* 6, 222-230.
- 418 Anpilov, A., Barkhudarov, E., Bark, Y.B., Zadiraka, Y.V., Christofi, M., Kozlov, Y.N.,
419 Kossyi, I., Kop'ev, V., Silakov, V., Taktakishvili, M., 2001. Electric discharge in water as a
420 source of UV radiation, ozone and hydrogen peroxide. *Journal of Physics D: Applied Physics*
421 34, 993.
- 422 Bansode, A.S., More, S.E., Siddiqui, E.A., Satpute, S., Ahmad, A., Bhoraskar, S.V., Mathe,
423 V.L., 2017. Effective degradation of organic water pollutants by atmospheric non-thermal
424 plasma torch and analysis of degradation process. *Chemosphere* 167, 396-405.
- 425 Clements, J.S., Sato, M., Davis, R.H., 1987. Preliminary investigation of prebreakdown
426 phenomena and chemical reactions using a pulsed high-voltage discharge in water. *IEEE*
427 *Transactions on industry applications*, 224-235.
- 428 Chandana, L., Reddy, P.M.K., Subrahmanyam, C., 2015. Atmospheric pressure non-thermal
429 plasma jet for the degradation of methylene blue in aqueous medium. *Chemical Engineering*
430 *Journal* 282, 116-122.
- 431 Deng, X., Nikiforov, A.Y., Vanraes, P., Leys, C., 2013. Direct current plasma jet at
432 atmospheric pressure operating in nitrogen and air. *Journal of Applied Physics* 113, 023305.
- 433 Dojčinović, B.P., Roglič, G.M., Obradović, B.M., Kuraica, M.M., Kostić, M.M., Nešić, J.,
434 Manojlović, D.D., 2011. Decolorization of reactive textile dyes using water falling film
435 dielectric barrier discharge. *Journal of hazardous materials* 192, 763-771.
- 436 Ferreira, C., Moisan, M., 1993. *Fundamentals and Applications*. Nato ASI Series, Series B,
437 *Physics* 302.
- 438 Foster, J., Sommers, B.S., Gucker, S.N., Blankson, I.M., Adamovsky, G., 2012. Perspectives
439 on the Interaction of Plasmas With Liquid Water for Water Purification. *IEEE Transactions*
440 *on Plasma Science* 40, 1311-1323.
- 441 Foster, J.E., Adamovsky, G., Gucker, S.N., Blankson, I.M., 2013. A comparative study of the
442 time-resolved decomposition of methylene blue dye under the action of a nanosecond
443 repetitively pulsed DBD plasma jet using liquid chromatography and spectrophotometry.
444 *IEEE Transactions on Plasma Science* 41, 503-512.
- 445 García, M., Varo, M., Martínez, P., 2010. Excitation of species in an expanded argon
446 microwave plasma at atmospheric pressure. *Plasma Chemistry and Plasma Processing* 30,
447 241-255.
- 448 Glaze, W.H., Kang, J.-W., Chapin, D.H., 1987. *The Chemistry of Water Treatment Processes*
449 *Involving Ozone, Hydrogen Peroxide and Ultraviolet Radiation*. *Ozone: Science &*
450 *Engineering* 9, 335-352.
- 451 Guo, H., Wang, H., Wu, Q., Zhou, G., Yi, C., 2016. Kinetic analysis of acid orange 7
452 degradation by pulsed discharge plasma combined with activated carbon and the synergistic
453 mechanism exploration. *Chemosphere* 159, 221-227.

454 Henriques, J., Tatarova, E., Dias, F., Ferreira, C., 2011a. Microwave N₂-Ar plasma torch. II.
455 Experiment and comparison with theory. *Journal of Applied Physics* 109, 023302.
456 Henriques, J., Tatarova, E., Ferreira, C., 2011b. Microwave N₂-Ar plasma torch. I. Modeling.
457 *Journal of Applied Physics* 109, 023301.
458 Huang, F., Chen, L., Wang, H., Yan, Z., 2010. Analysis of the degradation mechanism of
459 methylene blue by atmospheric pressure dielectric barrier discharge plasma. *Chemical
460 Engineering Journal* 162, 250-256.
461 Jackson, G.P., King, F.L., 2003. Probing excitation/ionization processes in millisecond-pulsed
462 glow discharges in argon through the addition of nitrogen. *Spectrochimica Acta Part B:
463 Atomic Spectroscopy* 58, 185-209.
464 Kim, K.-S., Kam, S.K., Mok, Y.S., 2015. Elucidation of the degradation pathways of
465 sulfonamide antibiotics in a dielectric barrier discharge plasma system. *Chemical Engineering
466 Journal* 271, 31-42.
467 Krugly, E., Martuzevicius, D., Tichonovas, M., Jankunaite, D., Rumskaitė, I., Sedlina, J.,
468 Racys, V., Baltrusaitis, J., 2015. Decomposition of 2-naphthol in water using a non-thermal
469 plasma reactor. *Chemical Engineering Journal* 260, 188-198.
470 Laroussi, M., 2009. Low-temperature plasmas for medicine? *IEEE Transactions on Plasma
471 Science* 37, 714-725.
472 Laroussi, M., Akan, T., 2007. Arc - Free Atmospheric Pressure Cold Plasma Jets: A Review.
473 *Plasma Processes and Polymers* 4, 777-788.
474 Lietz, A.M., Kushner, M.J., 2016. Air plasma treatment of liquid covered tissue: long
475 timescale chemistry. *Journal of Physics D: Applied Physics* 49, 425204.
476 Locke, B.R., Shih, K.-Y., 2011. Review of the methods to form hydrogen peroxide in
477 electrical discharge plasma with liquid water. *Plasma Sources Science and Technology* 20,
478 034006.
479 Lu, X., Laroussi, M., Puech, V., 2012. On atmospheric-pressure non-equilibrium plasma jets
480 and plasma bullets. *Plasma Sources Science and Technology* 21, 034005.
481 Lukes, P., Clupek, M., Babicky, V., Janda, V., Sunka, P., 2005. Generation of ozone by
482 pulsed corona discharge over water surface in hybrid gas-liquid electrical discharge reactor.
483 *Journal of Physics D: Applied Physics* 38, 409.
484 Lukes, P., Dolezalova, E., Sisrova, I., Clupek, M., 2014. Aqueous-phase chemistry and
485 bactericidal effects from an air discharge plasma in contact with water: evidence for the
486 formation of peroxyxynitrite through a pseudo-second-order post-discharge reaction of H₂O₂
487 and HNO₂. *Plasma Sources Science and Technology* 23, 015019.
488 Lukes, P., Locke, B.R., 2005. Plasmachemical oxidation processes in a hybrid gas-liquid
489 electrical discharge reactor. *Journal of Physics D: Applied Physics* 38, 4074.
490 Magureanu, M., Bradu, C., Piroi, D., Mandache, N.B., Parvulescu, V., 2013. Pulsed corona
491 discharge for degradation of methylene blue in water. *Plasma Chemistry and Plasma
492 Processing* 33, 51-64.
493 Magureanu, M., Mandache, N.B., Parvulescu, V.I., 2007. Degradation of organic dyes in
494 water by electrical discharges. *Plasma Chemistry and Plasma Processing* 27, 589-598.
495 Magureanu, M., Piroi, D., Gherendi, F., Mandache, N.B., Parvulescu, V., 2008.
496 Decomposition of methylene blue in water by corona discharges. *Plasma Chemistry and
497 Plasma Processing* 28, 677-688.
498 Magureanu, M., Piroi, D., Mandache, N., David, V., Medvedovici, A., Bradu, C., Parvulescu,
499 V., 2011. Degradation of antibiotics in water by non-thermal plasma treatment. *water research*
500 45, 3407-3416.
501 Malik, M.A., 2010. Water purification by plasmas: which reactors are most energy efficient?
502 *Plasma Chemistry and Plasma Processing* 30, 21-31.

503 Mohajerani, M., Mehrvar, M., Ein-Mozaffari, F., 2009. An overview of the integration of
504 advanced oxidation technologies and other processes for water and wastewater treatment. *Int J*
505 *Eng* 3, 120-146.

506 Moisan, M., Pelletier, J., 1992. *Microwave Induced Plasmas, Plasma Technology, Vol. 4.*
507 Elsevier Science Publishing, The Netherlands.

508 Mora, M., del Carmen García, M., Jiménez-Sanchidrián, C., Romero-Salguero, F.J., 2010.
509 Transformation of light paraffins in a microwave-induced plasma-based reactor at reduced
510 pressure. *international journal of hydrogen energy* 35, 4111-4122.

511 Mora, M., García, M.C., Jiménez - Sanchidrián, C., Romero - Salguero, F.J., 2011.
512 Selectivity Control in a Microwave Surface - Wave Plasma Reactor for Hydrocarbon
513 Conversion. *Plasma Processes and Polymers* 8, 709-717.

514 Park, J., Henins, I., Herrmann, H., Selwyn, G., Hicks, R., 2001. Discharge phenomena of an
515 atmospheric pressure radio-frequency capacitive plasma source. *Journal of Applied Physics*
516 89, 20-28.

517 Reddy, P.M.K., Raju, B.R., Karuppiah, J., Reddy, E.L., Subrahmanyam, C., 2013.
518 Degradation and mineralization of methylene blue by dielectric barrier discharge non-thermal
519 plasma reactor. *Chemical Engineering Journal* 217, 41-47.

520 Sato, K., Yasuoka, K., 2008. Pulsed discharge development in oxygen, argon, and helium
521 bubbles in water. *IEEE Transactions on Plasma Science* 36, 1144-1145.

522 Selwyn, G., Herrmann, H., Park, J., Henins, I., 2001. Materials processing using an
523 atmospheric pressure, RF-generated plasma source. *Contributions to Plasma Physics* 41, 610-
524 619.

525 Stratton, G.R., Bellona, C.L., Dai, F., Holsen, T.M., Thagard, S.M., 2015. Plasma-based water
526 treatment: conception and application of a new general principle for reactor design. *Chemical*
527 *Engineering Journal* 273, 543-550.

528 Sun, B., Sato, M., Clements, J., 2000. Oxidative processes occurring when pulsed high
529 voltage discharges degrade phenol in aqueous solution. *Environmental science & technology*
530 34, 509-513.

531 Sun, Y., Liu, Y., Li, R., Xue, G., Ognier, S., 2016. Degradation of reactive blue 19 by needle-
532 plate non-thermal plasma in different gas atmospheres: Kinetics and responsible active
533 species study assisted by CFD calculations. *Chemosphere* 155, 243-249.

534 Timmermans, E., Jonkers, J., Thomas, I., Rodero, A., Quintero, M., Sola, A., Gamero, A.,
535 Van Der Mullen, J., 1998. The behavior of molecules in microwave-induced plasmas studied
536 by optical emission spectroscopy. 1. Plasmas at atmospheric pressure. *Spectrochimica Acta*
537 *Part B: Atomic Spectroscopy* 53, 1553-1566.

538 Walsh, J.L., Iza, F., Janson, N.B., Law, V., Kong, M.G., 2010. Three distinct modes in a cold
539 atmospheric pressure plasma jet. *Journal of Physics D: Applied Physics* 43, 075201.

540 Walsh, J.L., Shi, J., Kong, M.G., 2006. Contrasting characteristics of pulsed and sinusoidal
541 cold atmospheric plasma jets. *Applied Physics Letters* 88, 171501.

542 Wang, X., Li, Z., Zeng, J., Zhang, X., Lei, L., 2013. Improvement of atmospheric water
543 surface discharge with water resistive barrier. *Plasma Chemistry and Plasma Processing* 33,
544 691-705.

545 Yang, B., Zhou, M., Lei, L., 2005. Synergistic effects of liquid and gas phase discharges using
546 pulsed high voltage for dyes degradation in the presence of oxygen. *Chemosphere* 60, 405-
547 411.

548 Yu, Q., Yasuda, H., 1998. An optical emission study on expanding low-temperature cascade
549 arc plasmas. *Plasma Chemistry and Plasma Processing* 18, 461-485.

550 Zhu, D., Jiang, L., Liu, R.-l., Chen, P., Lang, L., Feng, J.-w., Yuan, S.-j., Zhao, D.-y., 2014.
551 Wire-cylinder dielectric barrier discharge induced degradation of aqueous atrazine.
552 *Chemosphere* 117, 506-514.

553 Zille, A., Oliveira, F.R., Souto, A.P., 2015. Plasma treatment in textile industry. Plasma
554 Processes and Polymers 12, 98-131.
555
556

Table 1[Click here to download Table: Table 1.docx](#)**Table 1**Energy yield at 50 % conversion ($F_{Ar} = 1400$ sccm).

Dye concentration (ppm)	$Y_{50\%}$ (g/kWh)
5	0.296
50	0.033
100	0.018
250	0.007 ^a

^aMaximum value registered (50% conversion was not reached)

Figure 1
[Click here to download high resolution image](#)

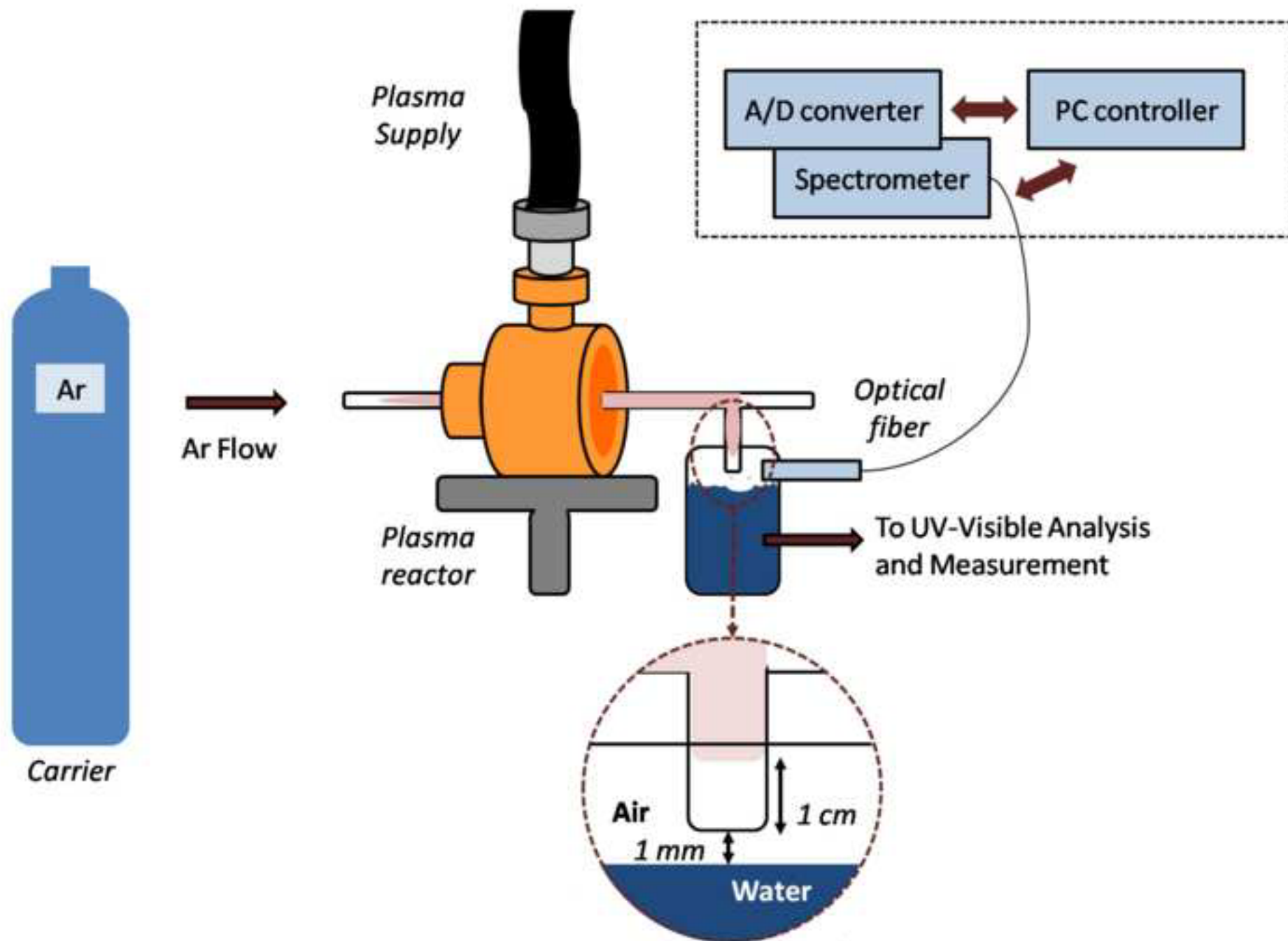


Figure 2
[Click here to download high resolution image](#)

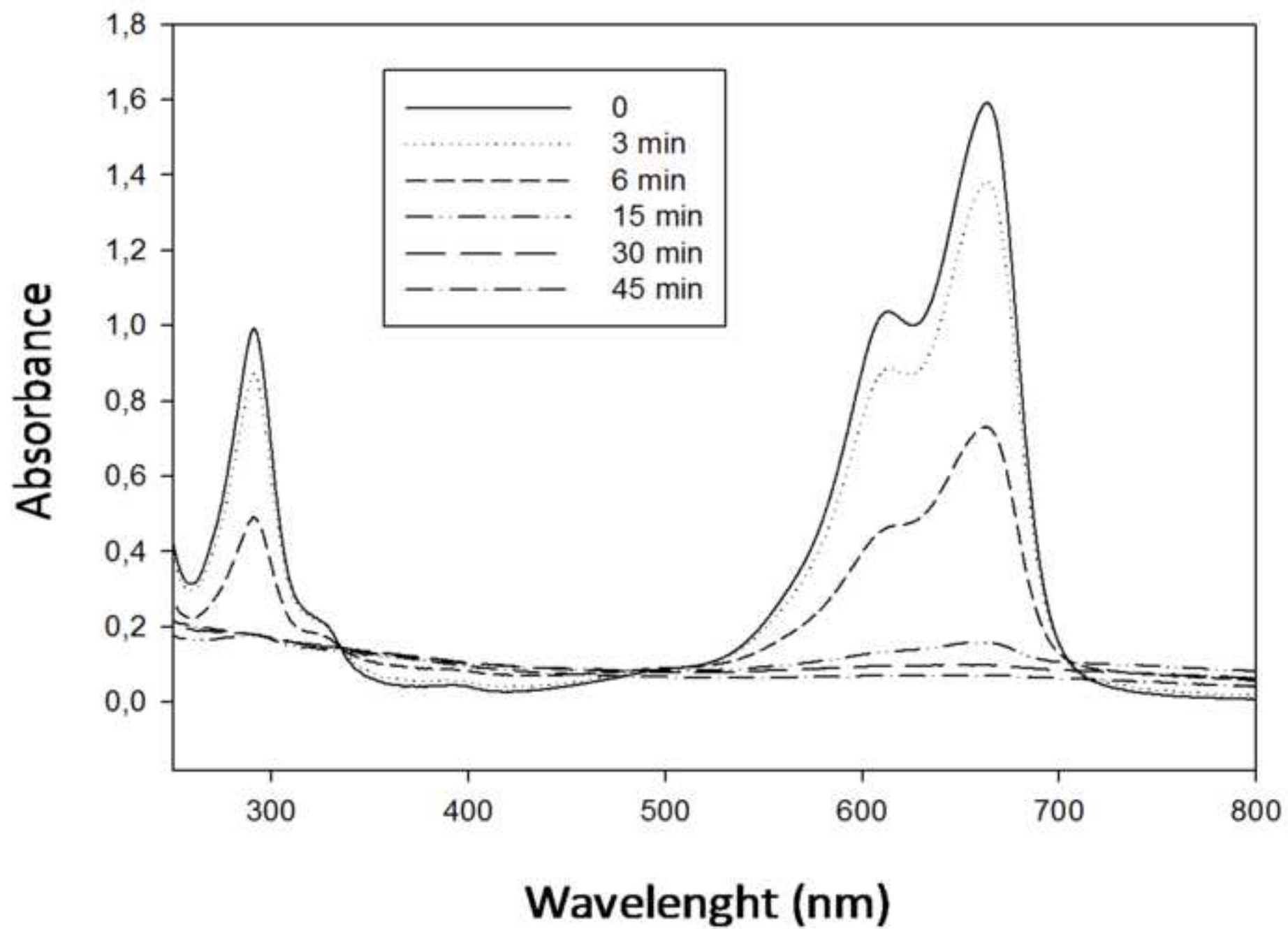


Figure 3
[Click here to download high resolution image](#)

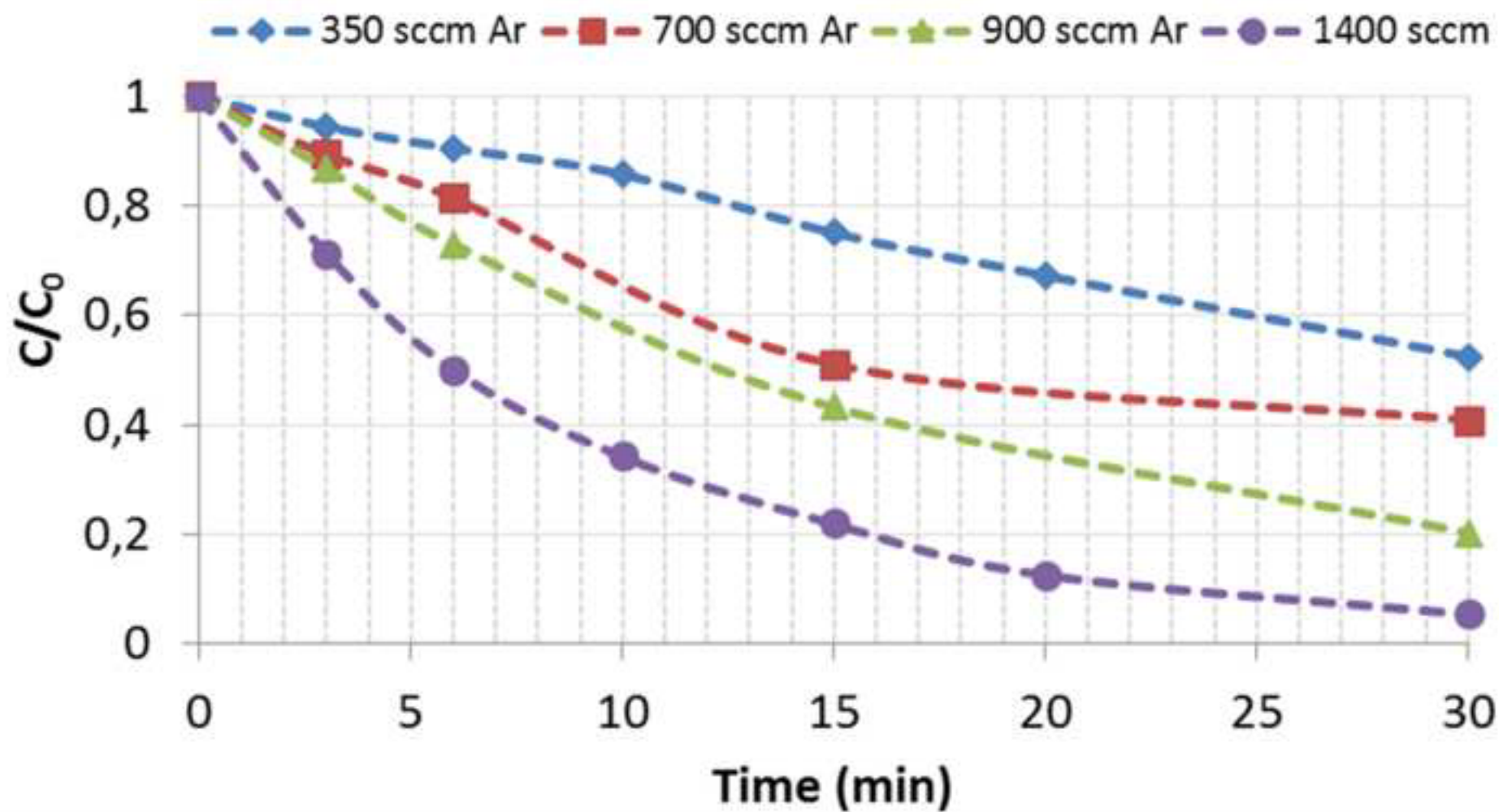


Figure 4
[Click here to download high resolution image](#)

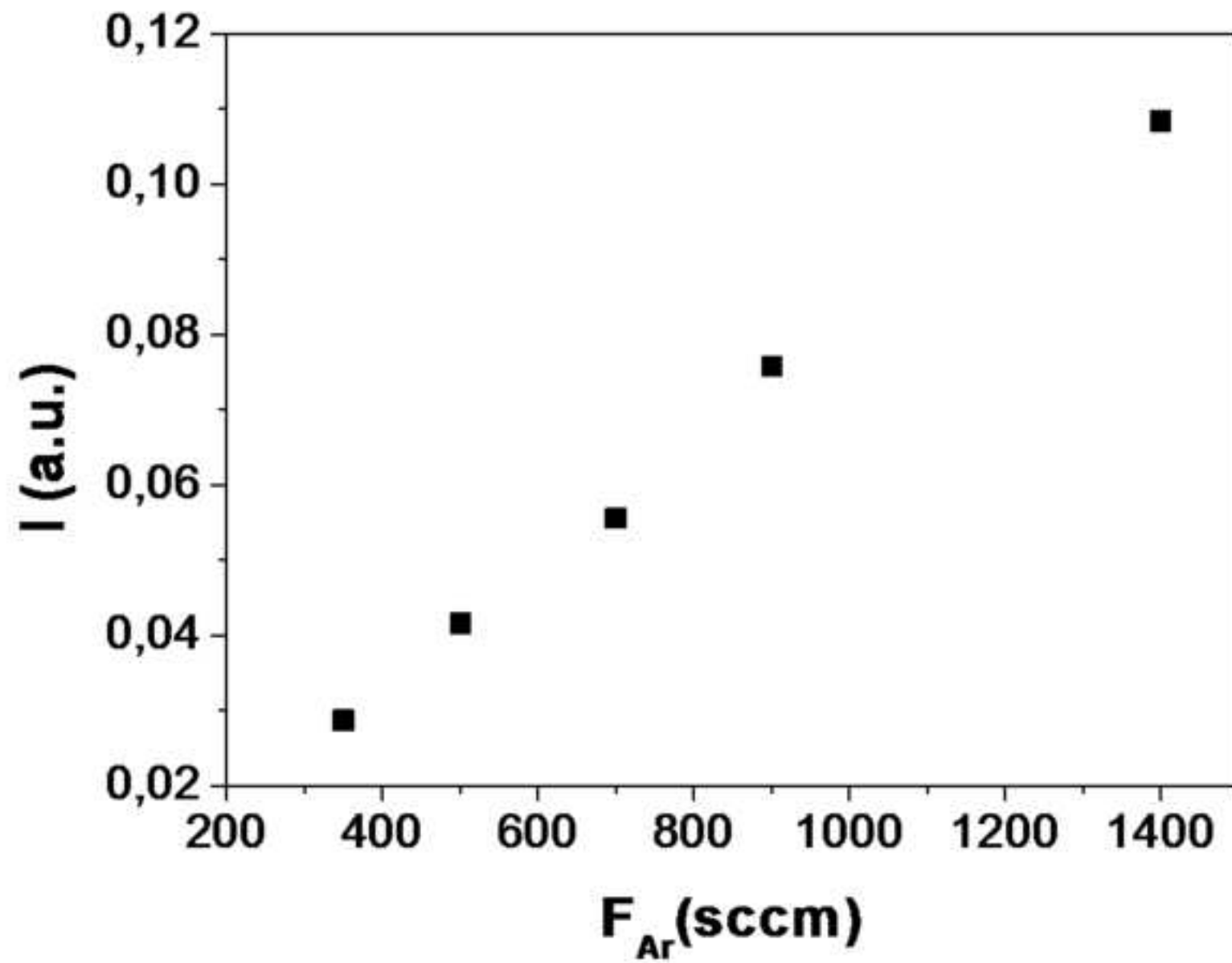


Figure 5
[Click here to download high resolution image](#)

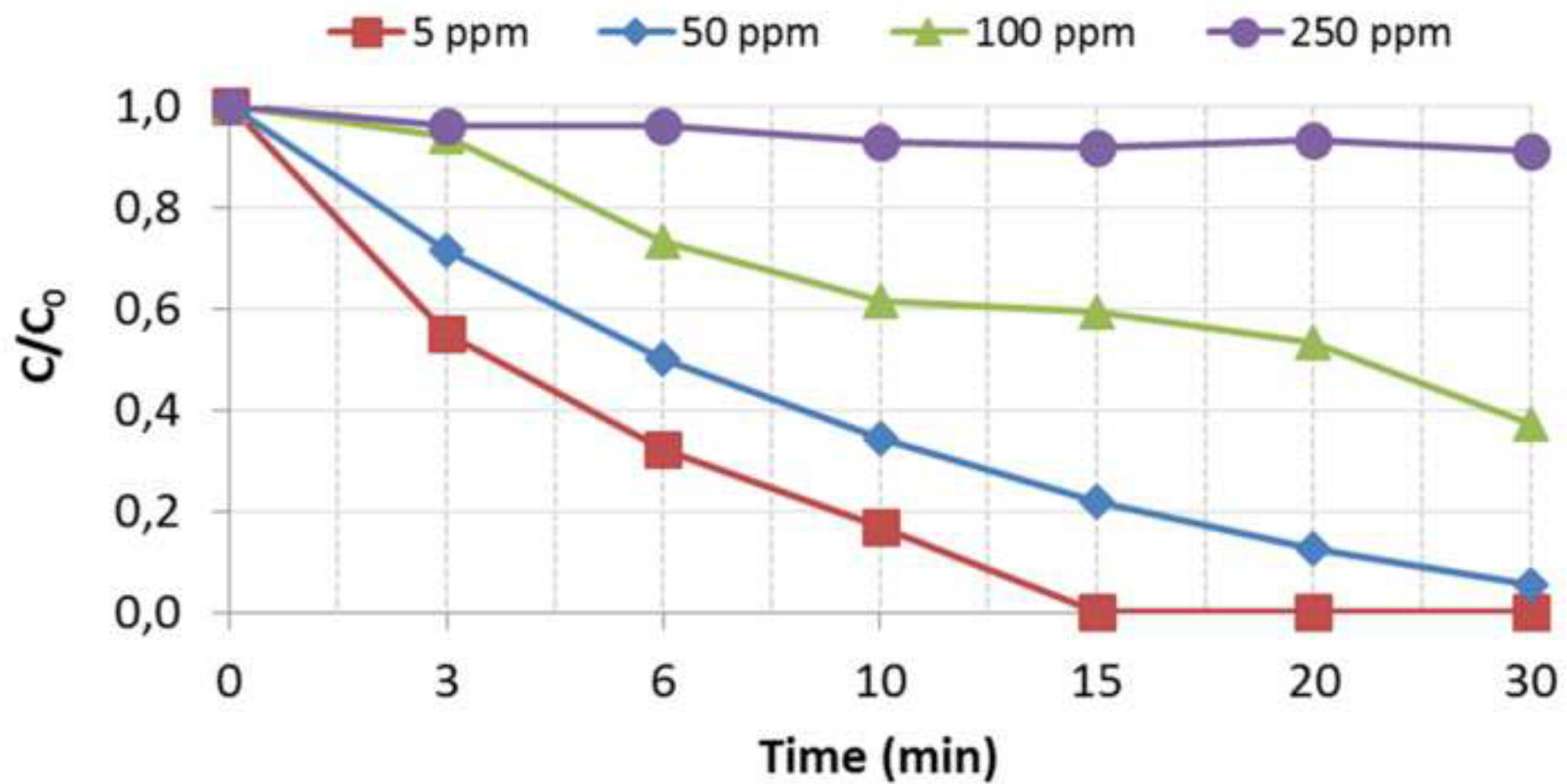


Figure 6
[Click here to download high resolution image](#)

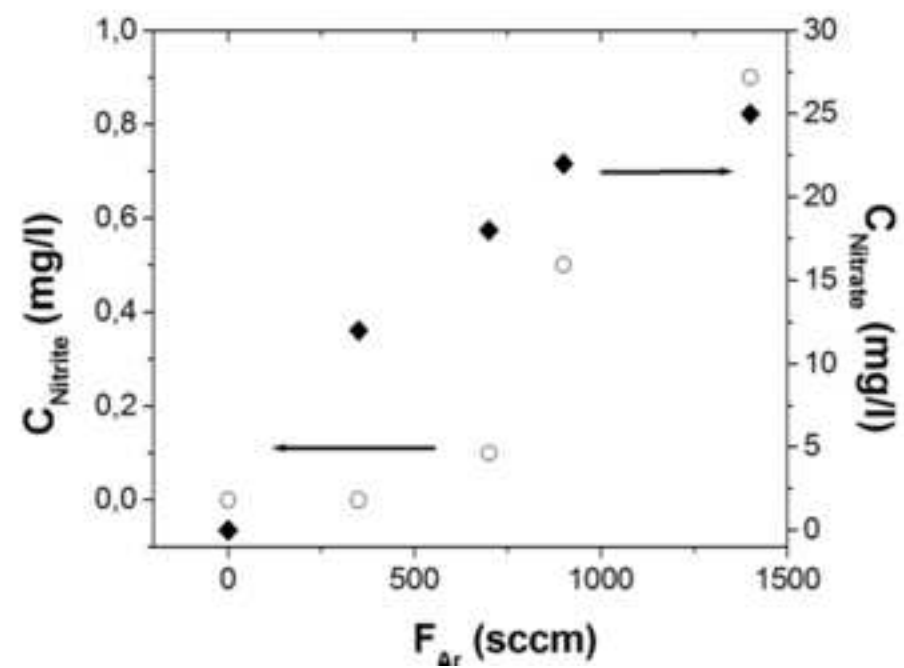
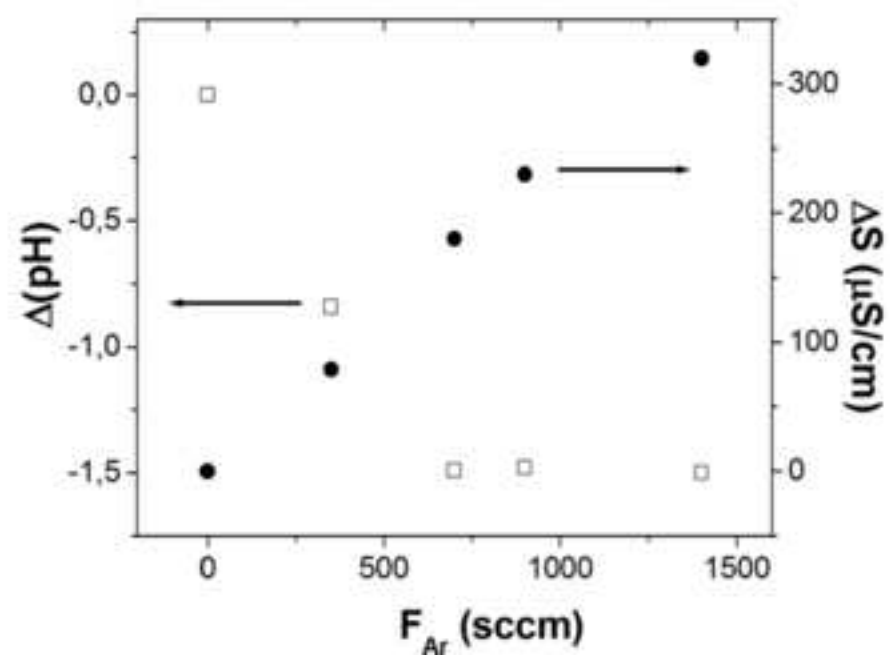


FIGURE CAPTIONS

Fig. 1. Experimental set-up for the generation of plasma and OES measurements

Fig. 2. UV–visible spectra for an untreated and plasma jet treated MB solution (50 ppm) during different time intervals

Fig. 3. Degradation of the dye over time (MB concentration 50 ppm) for plasma treatments using different argon flow rates

Fig. 4. Intensity of the Ar I line 763.51 nm measured next to the water for different argon flow rates

Fig. 5. Degradation of the dye over time for plasma treatments of MB aqueous solutions of different initial concentrations (argon flow rate 1400 sccm).

Fig. 6. Changes of electrical conductivity and pH (left) and concentrations of nitrite and nitrate (right) in water after plasma treatment as a function of argon flow rate

Supplementary Material

[Click here to download Supplementary Material: Garciaetal-Chemosphere-SM.docx](#)

